JTE HCMUTE
ISSN: 2615-9740

JOURNAL OF TECHNICAL EDUCATION SCIENCE
Ho Chi Minh City University of Technology and Education
Website: https://jte.hcmute.edu.vn/
Email: jte@hcmute.edu.vn

Global Analysis of Three-Dimensional Shape Symmetry: Human Heads (Part I)

Vi-Do Tran[1], Tien-Tuan Dao[2], Tan-Nhu Nguyen[1*]
[1]HCM City University of Technology and Education, Ho Chi Minh City, Vietnam
[2]Affiliation 3Univ. Lille, CNRS, Centrale Lille, UMR 9013 – LaMcube – Laboratoire de Mécanique, Multiphysique, Multiéchelle, 59655 Villeneuve d'Ascq Cedex, F-59000, Lille, France

[*] Corresponding author. *Email: nhunt@hcmute.edu.vn*

ARTICLE INFO

Received: 15/12/2021
Revised: 22/12/2021
Accepted: 25/1/2022
Published: 28/2/2022

KEYWORDS

Facial paralysis grading;
Global head symmetry;
Head distance symmetry;
Head volumetric symmetry;
Facial palsy detection.

ABSTRACT

Facial paralysis grading methods are mostly based on geometrical dissymmetry between left and right heads. Dissymmetry also appears even on healthy subjects. Consequently, this dissymmetry should be computed to distinguish with one on facial palsy patients. However, no studies have been quantitatively reported this characteristic. In the first part of our study, we tried to calculate this quantity by computing distance and volumetric differences between left and right heads. In particular, 329 head models were reconstructed from medical images of subjects with normal head geometries in neutral mimics. These heads were then automatically cut into left and right regions. Then, Hausdorff distances between left heads and mirrored right heads were computed. Moreover, volumetric differences between left head convex hulls and mirrored right head convex hulls were also calculated. As a result, the dissymmetry values (Mean ± SD) in mean Hausdorff distances are 1.8243 ± 0.7029 mm, and ones in volumetric are 78.1254 ± 65.7040 cm^3. In perspective, in the second part of our study, we will try to analyze geometrical symmetry on human skulls. Moreover, shape symmetry will be analyzed in more detail with different local shape topologies in different facial mimics. These analyses will finally be implemented on our clinical decision-support system for facial mimic rehabilitation.

Doi: https://doi.org/10.54644/jte.68.2022.1076

1. Introduction

Facial palsy negatively affected both the personal and social lives of involved patients [1]. Facial paralysis grading should be first conducted to evaluate the facial paralysis levels to propose suitable rehabilitation programs and to evaluate development progress [2]. Facial paralysis grading methods are classified into clinical and non-clinical grading systems [1] - [3]. Compared with clinical grading systems, the non-clinical ones have been increasingly interested due to their independence from subjective evaluation of clinicians [1] - [3]. However, the computed paralysis levels from the non-clinical methods still need to be assessed by clinicians to detect facial palsy [1] - [3].

Non-clinical facial paralysis grading, which mainly based on computer-aided processing methods for analyzing static (or dynamic) facial appearances in both 2-dimensional (2-D) and 3-dimensional (3-D) spaces [4]. However, 3-D non-clinical facial paralysis grading was more accurate and more robust than 2-D non-clinical facial paralysis grading. In particular, regarding the 2-D grading methods, mono cameras were usually used for capturing Red-Green-Blue (RGB) images of the subject with (or without) facial markers [5]. The gray levels (or landmark 2-D positions) on the left facial images were compared with ones on the right facial images through pixel values differences [5] (or 2-D location displacements of facial markers [6,7]). Although these grading methods were fast and simple, the grading results might be varied in light conditions [5], and they could not measure 3-D geometrical information [6]. 3-D information is important to evaluate the facial mimics, as they are the 3-D deformation results on the facial skin of muscle actions [8] - [10]. Regarding the 3-D grading methods, 3-D geometrical structures of the face (or 3-D positions of facial landmarks) could be captured (reconstructed) using 3-D capturing (scanning) devices, such as multiple camera systems [11] - [14], RGB-Depth sensors [15] - [16], laser

scanners [17] - [18], etc., straightforwardly. These devices could reach an accuracy from 0.13 mm to 1.0 mm and real-time framerates (up to 40 frames per second (FPS)) [19]. In the 3-D grading methods, geometrical structures on the left facial model (or landmark 3-D positions) were compared with ones on the right facial model using 3-D Euclidean distances [18], [20], [21] (or motion analysis methods [6] - [7]). These grading methods were not dependent on light conditions, and they can capture 3-D geometrical structures (movements) of the face. Recently, in our previous study, 3-D head models could be fast generated and tracked in real-time with animated facial texture based on the Kinect V2.0 sensors coupled with the concept of the system of systems [4].

In 3-D non-clinical facial paralysis grading methods, geometrical dissymmetry between left and right heads was computed as the facial paralysis levels [6], [7], [26], [12], [14], [18], [21] - [25]. Even in the normal subjects, muscle action line lengths in left and right head regions were even not symmetrical [4]. Moreover, muscle lengths were affected by both head and skull geometrical structures, as they were formed by the attachment points on the skull and the insertion points on the head [8–10]. Additionally, Hausdorff distance and volumetric differences between the left and right head regions were one of the most popular features for facial paralysis grading [4], [18], [20], [21]. Consequently, the geometrical dissymmetry is valuable to be analyzed and reported in a quantitative manner for the normal subjects. These dissymmetrical values could be used to compare with ones computed by non-clinical facial paralysis grading [4], [18], [20], [21] to detect facial palsy automatically. Moreover, these values will be applied to our previous clinical decision-support system for facial mimic rehabilitation [27]. They will be used as dissymmetrical thresholds for automatically diagnosing facial palsy. However, up to now, no studies have been reported these values.

Consequently, this present study tried to analyze and report geometrical dissymmetry levels of normal human heads. In particular, 329 three-dimensional (3-D) head models reconstructed from medical images of subjects having normal head structures were processed and cut into left and right regions. The left and right head regions were then mirrored to the right and left through a middle plane using reflecting transforms. Hausdorff distances between the left head regions and the mirrored right head regions were computed. Moreover, the volumetric differences between left head convex hulls and mirrored right head convex hulls were also reported.

As a result, the distance dissymmetry values (Mean ± SD) are 1.8243 ± 0.7029 mm, and the volumetric dissymmetry values (Mean ± SD) are 78.1254 ± 65.7040 cm^3. These values could be applied in facial paralysis grading in automatic detection of facial palsy.

In perspective, with the same computing techniques, we will compute the geometrical symmetry of the human skull in the second part of our study. Moreover, the head and skull symmetry will be analyzed in more detail with local topological shapes in different facial mimics. These global and local symmetries will be implemented in our clinical decision support system for facial mimic rehabilitation [27].

In the following, we will explain in detail the analyzing methods in Section 2. Distance and volumetric symmetry levels will also be reported in Section 3. Conclusions and perspectives of this paper will be presented in Section 4.

2. Materials and Methods

2.1. Datasets

Three hundred and twenty-nine head models were manually reconstructed from DICOM [512 × 512] Computed Tomography (CT) images of 329 subjects (male: 265, female: 64, ages (Mean ± SD): 61 ± 11 years), which have normal head geometries. The CT images were collected from The Cancer Imaging Archive (TCIA) [28]. The CT images of each subject were reconstructed and post-processed to keep only the head regions using the 3DSlicer [29] and MeshLab [30].

Details of model reconstruction and post-processing were presented in our previous study [31]. We will describe briefly here the model reconstruction procedure. First, 2-D CT images were selected so that they contain both head and neck regions. The head segments were then selected by choosing suitable

gray levels of DICOM images using the gray level selection tool in the 3DSclicer software [29]. 2-D head segments were reconstructed into 3-D head models using the marching cube algorithm in 3DSlicer [29]. The reconstructed head models were then cut and re-meshed so that only the head regions were in the dataset. The cutting and re-meshing procedures were conducted using the mesh processing tools in MeshLab [30].

After reconstruction, the volumes (Mean ± SD) of the head models are 1,412.34 ± 284.23 cm^3. The head volumes were computed using an open-source function (i.e. FT CGAL::Polygon_mesh_processing::volume) in the CGAL library [32]. It is important to note that all subjects had CT scanning when they were in neutral mimics.

2.2. Overall Processing Procedure

The overall analysis procedure is illustrated in Figure 1. In particular, all 329 head models were first registered to the same coordinate system of a template head model. The template head model was fixed so that it was aligned with the global x-, y-, and z-axes in the vertical orientation. The left and right head regions were then cut from the full head models of all subjects. The left & right heads were mirrored through the center planes of the head models. Hausdorff distance [33] between the left head regions and the mirrored right head regions (and vice versa, between the right head regions and the mirrored left head regions) was computed for the distance symmetry analysis. Moreover, volumetric differences between the left head convex hulls and the mirrored right head convex hulls (and vice versa, between the right head convex hulls and the mirrored left head convex hulls) were also computed for the volumetric symmetry analysis.

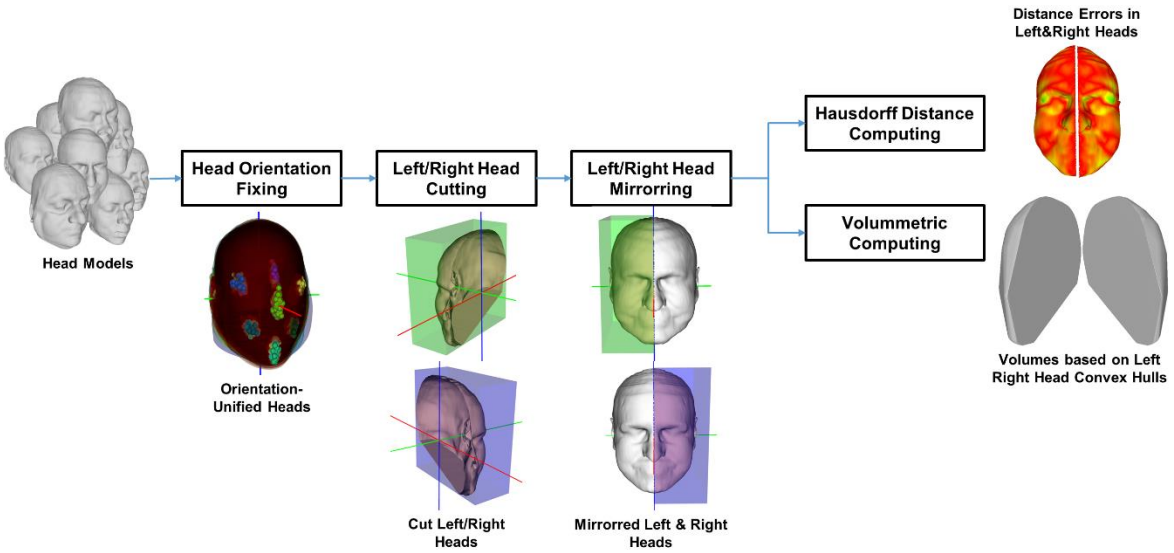

Figure 1. *Overall analysis procedure of the head geometrical symmetry computing*

2.3. Head Orientation Fixing

To minimize the rigid differences among the head models in the dataset, all head models were registered to the same coordinate system of the template head model. The template head model (Figure 2a), which was used in our previous study [27], was exactly symmetrical between the left and right regions. This model was fixed so that the left and right tragions were aligned with the y-axis, and the pronasale was on the x-axis (Figure 2b). This procedure will make the template head exactly be in the vertical direction. The head models of all subjects were then registered to the template head using the singular value decomposition (SVD) rigid registration method [34] based on the feature points: left & right exocanthions, nasion, pronasale, left & right cheilion, and gnathion (Figure 2c). These points were manually selected on the whole head dataset. To minimized the manual selection of the key points, the rigid coherent point drift (CPD) [35] registration method was finally employed on all vertices of the subject head and the template head. This registration method will find the probabilistically optimal rigid

JTE
HCMUTE
ISSN: 2615-9740

JOURNAL OF TECHNICAL EDUCATION SCIENCE
Ho Chi Minh City University of Technology and Education
Website: https://jte.hcmute.edu.vn/
Email: jte@hcmute.edu.vn

transforms to rigidly fit the subject head to the template head [35]. As a result, all head models were optimally on the same coordinate system with the template head (Figure 2d).

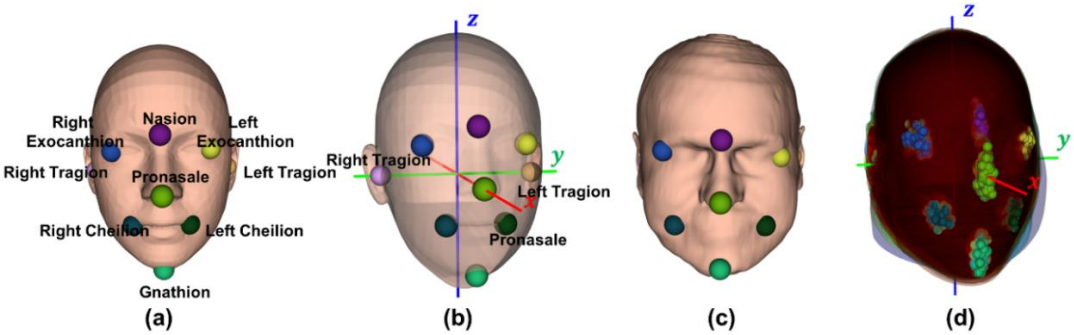

Figure 2. *Head models and feature points for minimizing rigid-differences: (a) a template head with its feature points; (b) the orientation-fixed template head; (c) a subject head with its feature points; and (d) all registered head models on the same coordinate system with the template head.*

2.4. Estimation of ROI Boxes and Left & Right Head Cutting

All registered head models were cut into left and right regions using the bounding box-based method. In particular, for each head in the dataset, a bounding box was estimated so that it covered all vertices of the head model (Figure 3a). The left bounding box was defined as the half-left part of the full bounding box (Figure 3b, d), and the right bounding box was defined as the half-right part of the full bounding box (Figure 3c, d). The left head region has vertices and facets that were inside the left bounding box (Figure 3e), and the right head region has vertices and facets that were inside the right bounding box (Figure 3f).

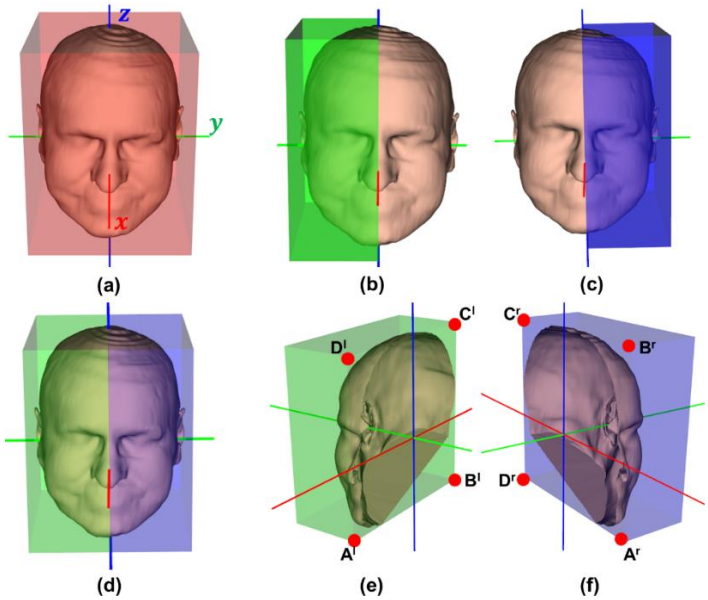

Figure 3. *Bounding boxes estimating and left & right head cutting: (a) full bounding box; (b) left bounding box; (c) right bounding box; (d) left & right bounding boxes in the same coordinate system; (e) left head region inside the left bounding box; and (f) the right head region inside the right bounding box.*

2.5. Left & Right Head Mirroring

The left and right head regions of each subject were mirrored through the center plane of the full bounding box. The center plane was defined as (A^l B^l C^l D^l) or (A^r B^r C^r D^r). In which, A^l, B^l, C^l, D^l, A^r, B^r, C^r, and D^r are the four corners of the left (l) bounding boxes (Figure 3e) and the right (r) bounding box (Figure 3f). The reflecting Householder transform [36] was used to mirror the left head region and the right head region to form the mirrored left head region (Figure 4a) and the mirrored right head region (Figure 4b), respectively.

JTE
HCMUTE
ISSN: 2615-9740

JOURNAL OF TECHNICAL EDUCATION SCIENCE
Ho Chi Minh City University of Technology and Education
Website: https://jte.hcmute.edu.vn/
Email: jte@hcmute.edu.vn

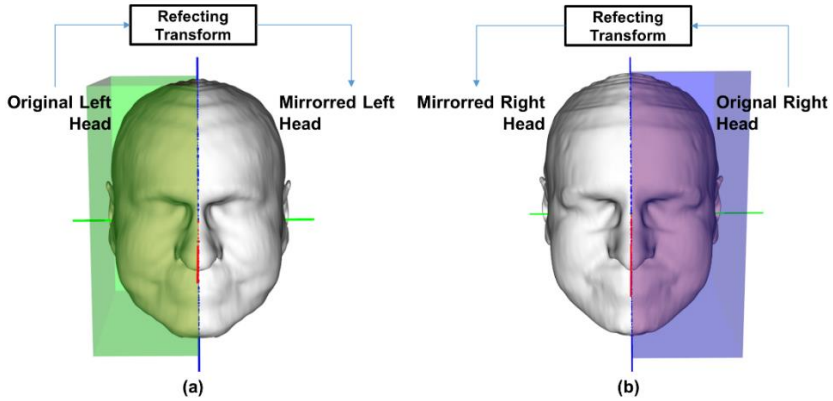

Figure 4. *Left & right head mirroring using the reflecting Householder transform* [36]*: (a) the mirrored left head was mirrored from the left head; (b) the mirrored right head was mirrored from the right head.*

2.6. Distance Symmetry Analysis

The left head model will be compared with the mirrored right head model using the Hausdorff distance metric [33]. In this metric, shape differences between the two surface models are represented as Euclidean distances between the vertices in the first model and their nearest vertices in the second model, as shown in Figure 5a. It is important to note that, in the dataset, all head models were post-processed to have the same number of vertices as each other [31]. Consequently, the Hausdorff distance could be used to represent for left & right head symmetrical level. In this paper, we report the distance asymmetrical level as mean Hausdorff distances. Additionally, Hausdorff distances between the right head and the mirrored left head were also computed (Figure 5b).

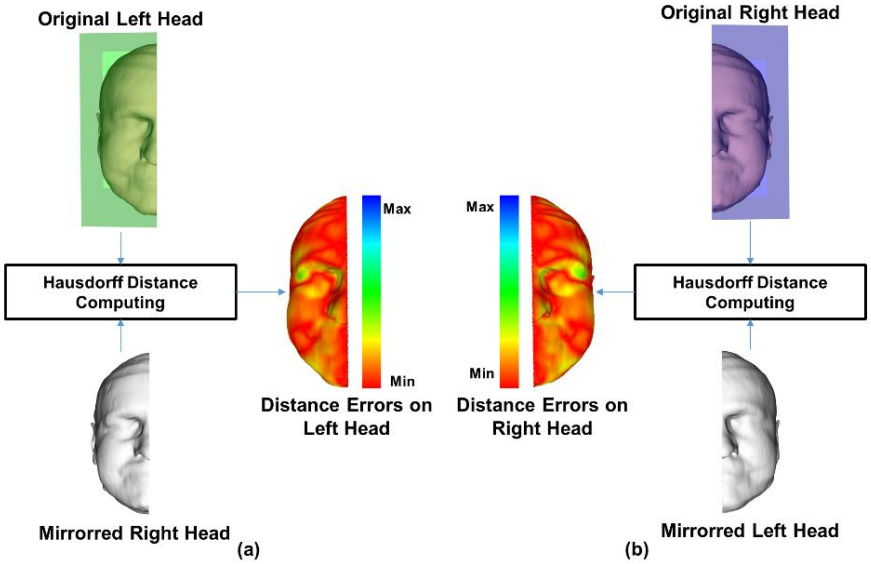

Figure 5. *Distance symmetrical level computing: (a) between the left heads and the mirrored right heads; (b) between the right heads and the mirrored left heads.*

2.7. Volumetric Symmetry Analysis

To analyze volumetric symmetry levels, the volumes of the left, mirrored left, right, and mirrored right head convex hulls were computed. Volumetric symmetry levels among the surface models could be represented as the volumetric symmetry level among their convex hulls. In this study, as presented in Figure 6, we computed volumetric differences between the left head convex hulls and the mirrored right head convex hulls as the volumetric symmetry levels. Moreover, the volumetric differences between the right head convex hulls and the mirrored left convex hulls were also computed.

JTE
HCMUTE
ISSN: 2615-9740

JOURNAL OF TECHNICAL EDUCATION SCIENCE
Ho Chi Minh City University of Technology and Education
Website: https://jte.hcmute.edu.vn/
Email: jte@hcmute.edu.vn

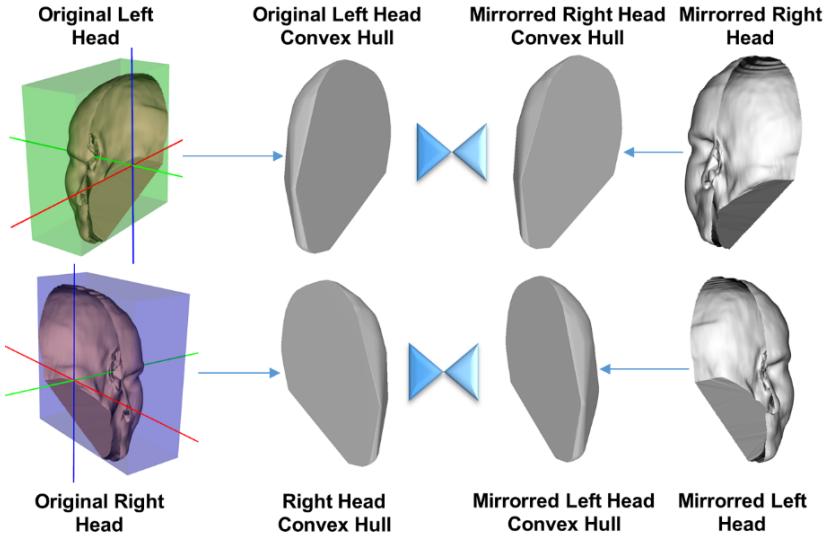

Figure 6. *Volumetric symmetry computed from the left (right) head convex hulls and mirrored right (left) head convex hulls.*

3. Results and Discussion

Figure 7 shows the distance and volumetric symmetry levels of the human heads computed from the whole dataset. As shown in Figure 7a, the mean Hausdorff distances (Mean ± SD) between the left heads and mirrored right heads are 1.8243 ± 0.7029 mm, and between the right heads and the mirrored left heads are 1.8692 ± 0.7377 mm. It is important to know that distances errors between the left heads and the mirrored right heads are approximately the same as ones between the right heads and the mirrored left heads. Regarding the volumetric symmetry levels, as shown in Figure 7b, the volumetric differences between the left head convex hulls and the mirrored right head convex hulls are the same as ones between the right head convex hulls and the mirrored left head convex hulls. These values (Mean ± SD) are 78.1254 ± 65.7039 cm^3. Consequently, to analyze the symmetrical levels of human heads, we just need to compare one side (left/right) and the mirrored version from the other side of the head.

Overall, based on the computed results, even the healthy subjects, which do not have great abnormal appearances on their heads, their left and right head regions are not perfectly symmetrical both in distance and in volumetric geometries. The reported values are meaningful to non-clinical facial paralysis grading methods that mainly used symmetrical values between the left and right head regions to evaluate facial paralysis. In particular, in these studies, face models were compared with their horizontally mirrored models using Hausdorff distances to output a facial paralysis score [18]. This score will then be evaluated by clinicians to conclude the status of facial palsy of their patient(s) based on their experiences [2]. However, with recent increasing requirements for home telehealth, these diagnosis processes need to be conducted automatically [37]. Based on the results of this study, facial paralysis could be automatically diagnosis by comparing the current paralysis levels with the reported values. Moreover, in our previous study, the muscle action lengths were computed for both left and right sides on healthy subjects [4], and we realized that even in the healthy subjects the muscle lengths in neutral mimics are not perfectly symmetrical between the left and right sides. Consequently, the reported values in the present study help us partially explain that this dissymmetry of the muscle action lengths comes from the dissymmetry of the head in the neutral mimic.

However, it is important to note that in this study we just analyzed and reported the geometrical symmetries (including Hausdorff distance and volumetric differences) of the normal heads of healthy subjects in neutral facial mimics. The reported values will become the normal thresholds for automatically diagnosing the ab-normal facial appearances.

In perspective, we will apply the same processing techniques for computing geometrical symmetry for human skulls in the second part of our study. Moreover, head and skull symmetries will be analyzed

JTE HCMUTE
ISSN: 2615-9740
JOURNAL OF TECHNICAL EDUCATION SCIENCE
Ho Chi Minh City University of Technology and Education
Website: https://jte.hcmute.edu.vn/
Email: jte@hcmute.edu.vn

in more detail with local topological regions (e.g. eyes, mouth, ears, chin, and checks). Additionally, the geometrical symmetries will be examined in different facial mimics (e.g. smiling, and kissing). This will help automatically diagnose facial palsy in a dynamic manner. Finally, all the reported symmetrical values including both global and local topological regions will be implemented in our clinical decision support system for facial mimic rehabilitation [27].

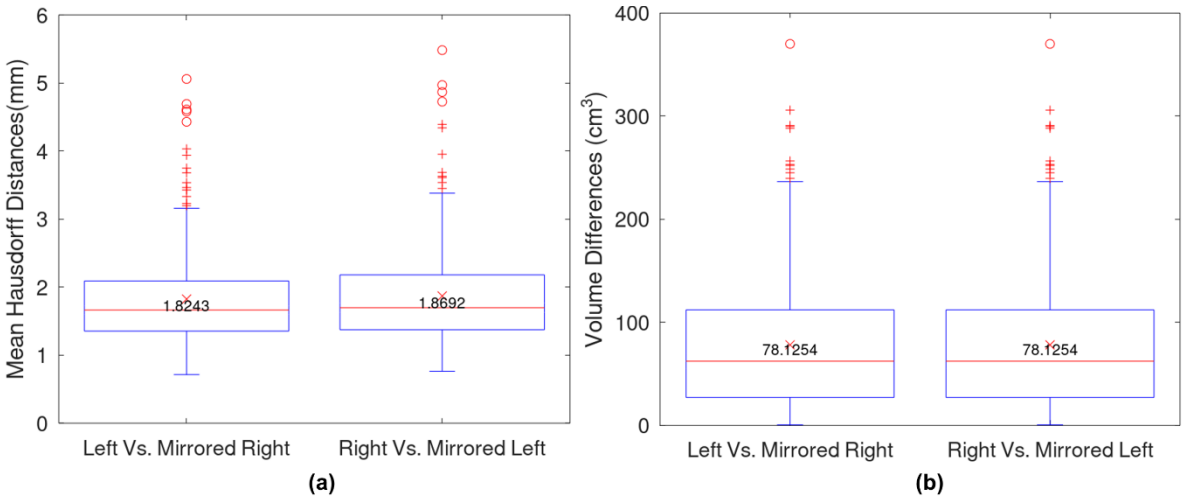

Figure 7. *Geometrical symmetry levels of human heads in the whole dataset: (a) Hausdorff distance dissymmetry between left and mirrored right heads and between right and mirrored left heads; (b) volumetric dissymmetry between left and mirrored right head convex hulls and between the right and mirrored left convex hulls.*

4. Conclusions

In this study, we reported the distance and volumetric symmetrical values of the human head. Base on the dataset of 329 healthy subjects, the distance dissymmetrical values (Mean ± SD) are 1.8243 ± 0.7029 mm, and the volumetric dissymmetrical values (Mean ± SD) are 78.1254 ± 65.7039 cm^3. These values are important to automatic facial paralysis grading. In perspective, the symmetrical analysis will be conducted on local topologies and in various facial mimics for both head and skulls. Both local and global dissymmetrical analyses will be implemented in our clinical decision support system for facial mimic rehabilitation [27].

Acknowledgments

This work belongs to the project grant No: B2022-SPK-01 funded by Ministry of Education and Training, and hosted by Ho Chi Minh City University of Technology and Education, Vietnam.

REFERENCES

[1] W.S.W. Samsudin and K. Sundaraj, Clinical and non-clinical initial assessment of facial nerve paralysis: A qualitative review, Biocybern. Biomed. Eng. 34 (2014) 71–78. https://doi.org/10.1016/j.bbe.2014.02.005.

[2] M.W. Robinson and J. Baiungo, "Facial Rehabilitation: Evaluation and Treatment Strategies for the Patient with Facial Palsy," *Otolaryngol. Clin. North Am.*, vol.51, pp.1151–1167, 2018. https://doi.org/10.1016/j.otc.2018.07.011.

[3] A.Y. Fattah, A.D.R. Gurusinghe, J. Gavilan, T.A. Hadlock, J.R. Marcus, H. Marres, and et al, "Facial Nerve Grading Instruments," *Plast. Reconstr. Surg.*, vol.135, pp.569–579, 2015, https://doi.org/10.1097/PRS.0000000000000905.

[4] T.-N. Nguyen, S. Dakpe, M.-C. Ho Ba Tho, and T.-T. Dao, "Kinect-driven Patient-specific Head, Skull, and Muscle Network Modelling for Facial Palsy Patients," *Comput. Methods Programs Biomed.*, vol.200, 105846, 2021, https://doi.org/10.1016/j.cmpb.2020.105846.

[5] S. Wang, H. Li, F. Qi, and Y. Zhao, "Objective facial paralysis grading based onP face and eigenflow," *Med. Biol. Eng. Comput.*, vol.42 pp. 598–603, 2004, https://doi.org/10.1007/BF02347540.

[6] M. Frey, C.H. John Tzou, M. Michaelidou, I. Pona, A. Hold, E. Placheta, and et al, "3D Video Analysis of Facial Movements," *Facial Plast. Surg. Clin. North Am.*, vol.19,pp. 639–646, 2011, https://doi.org/10.1016/j.fsc.2011.07.007.

[7] M.D. Salgado, S. Curtiss, and T.T. Tollefson, "Evaluating symmetry and facial motion using 3D videography," *Facial Plast. Surg. Clin. North Am.*, vol.18, pp. 351–356, 2010, https://doi.org/10.1016/j.fsc.2010.01.011.

[8] T. Wu, A.P.L. Hung, P. Hunter, and K. Mithraratne, "Modelling facial expressions: A framework for simulating nonlinear soft tissue deformations using embedded 3D muscles," *Finite Elem. Anal. Des.*, vol.76, pp. 63–70, 2013, https://doi.org/10.1016/j.finel.2013.08.002.

[9] A.X. Fan, S. Dakpé, T.T. Dao, P. Pouletaut, M. Rachik, and M.C. Ho Ba Tho, "MRI-based finite element modeling of facial mimics: a case study on the paired zygomaticus major muscles," *Comput. Methods Biomech. Biomed. Engin.*, vol.20, pp.919–928, 2017, https://doi.org/10.1080/10255842.2017.1305363.

[10] T.T. Dao, A.X. Fan, S. Dakpé, P. Pouletaut, M. Rachik, and M.C. Ho Ba Tho, "Image-based skeletal muscle coordination: case study on a subject specific facial mimic simulation," *J. Mech. Med. Biol.*, vol.18, pp.1–15, 2018, https://doi.org/10.1142/S0219519418500203.
[11] T. Al-Anezi, B. Khambay, M.J. Peng, E. O'Leary, X. Ju, and A. Ayoub, "A new method for automatic tracking of facial landmarks in 3D motion captured images (4D)," *Int. J. Oral Maxillofac. Surg.*, vol.42, pp.9–18, 2013. https://doi.org/10.1016/j.ijom.2012.10.035.
[12] C.A. Trotman, J. Faraway, T. Hadlock, C. Banks, N. Jowett, and H.J. Jung, "Facial soft-tissue mobility: Baseline dynamics of patients with unilateral facial paralysis," *Plast. Reconstr. Surg. - Glob. Open.*, vol.6, pp.1–12, 2018, https://doi.org/10.1097/GOX.0000000000001955.
[13] K. Mishima and T. Sugahara, "Analysis methods for facial motion," *Jpn. Dent. Sci. Rev.*, vol.45, pp. 4–13, 2009, https://doi.org/10.1016/j.jdsr.2009.03.003.
[14] B. Hontanilla and C. Aubá, "Automatic three-dimensional quantitative analysis for evaluation of facial movement," *J. Plast. Reconstr. Aesthetic Surg.*, vol.61, pp. 18–30, 2008, https://doi.org/10.1016/j.bjps.2007.03.037.
[15] Z. Zhang, "Microsoft kinect sensor and its effect," *IEEE Multimed.*, vol.19, pp.4–10, 2012, https://doi.org/10.1109/MMUL.2012.24.
[16] R. C. Carro, E. B. Huerta, F. R. Cruz, R. M. Caporal, and C. P. Corona, "Facial Expression Analysis with Kinect for the Diagnosis of Paralysis Using Nottingham Grading System," *IEEE Lat. Am. Trans.*, vol.14, pp.3418–3426, 2016, https://doi.org/10.1109/TLA.2016.7587650.
[17] C. Jiang, J. Wu, W. Zhong, M. Wei, J. Tong, H. Yu, and L. Wang, "Automatic Facial Paralysis Assessment via Computational Image Analysis," *J. Healthc. Eng.*, vol.2020, 2020, https://doi.org/10.1155/2020/2398542.
[18] P.A. Desrosiers, Y. Bennis, M. Daoudi, B. Ben Amor, and P. Guerreschi, "Analyzing of facial paralysis by shape analysis of 3D face sequences," *Image Vis. Comput.*, vol.67, pp. 67–88, 2017, https://doi.org/10.1016/j.imavis.2017.08.006.
[19] C.-H.J. Tzou, N.M. Artner, I. Pona, A. Hold, E. Placheta, W.G. Kropatsch, and et al, "Comparison of three-dimensional surface-imaging systems," *J. Plast. Reconstr. Aesthetic Surg.*, vol.67, pp. 489–497, 2014, https://doi.org/10.1016/j.bjps.2014.01.003.
[20] D. Gibelli, D. De Angelis, P. Poppa, C. Sforza, and C. Cattaneo, "An Assessment of How Facial Mimicry Can Change Facial Morphology: Implications for Identification," *J. Forensic Sci.*, vol.62, pp. 405–410, 2017, https://doi.org/10.1111/1556-4029.13295.
[21] C. Tanikawa and K. Takada, "Test-retest reliability of smile tasks using three-dimensional facial topography," *Angle Orthod.*, vol.88, pp. 319–328, 2018, https://doi.org/10.2319/062617-425.1.
[22] C.-A. Trotman, C. Phillips, J.J. Faraway, and K. Ritter, "Association between Subjective and Objective Measures of Lip Form and Function: An Exploratory Analysis," *Cleft Palate-Craniofacial J.*, vol.40, pp.241–248, 2003, https://doi.org/10.1597/1545-1569_2003_040_0241_absaom_2.0.co_2.
[23] A. Al-Hiyali, A. Ayoub, X. Ju, M. Almuzian, and T. Al-Anezi, "The Impact of Orthognathic Surgery on Facial Expressions," *J. Oral Maxillofac. Surg.*, vol.73, pp. 2380–2390, 2015, https://doi.org/10.1016/j.joms.2015.05.008.
[24] H. Popat, E. Henley, S. Richmond, L. Benedikt, D. Marshall, and P.L. Rosin, "A comparison of the reproducibility of verbal and nonverbal facial gestures using three-dimensional motion analysis," *Otolaryngol. - Head Neck Surg.*, vol.142, pp.867–872, 2010, https://doi.org/10.1016/j.otohns.2010.03.003.
[25] K. Mishima, H. Umeda, A. Nakano, R. Shiraishi, S. Hori, and Y. Ueyama, "Three-dimensional intra-rater and inter-rater reliability during a posed smile using a video-based motion analyzing system," *J. Cranio-Maxillofacial Surg.*, vol.42, pp.428–431, 2014, https://doi.org/10.1016/j.jcms.2013.05.035.
[26] C.A. Trotman, J. Faraway, and T.A. Hadlock, "Facial mobility and recovery in patients with unilateral facial paralysis," Orthod. Craniofacial Res., vol.23, pp. 82–91, 2020, https://doi.org/10.1111/ocr.12346.
[27] T.-N. Nguyen, S. Dakpé, M.-C. Ho Ba Tho, and T.-T. Dao, "Real-time computer vision system for tracking simultaneously subject-specific rigid head and non-rigid facial mimic movements using a contactless sensor and system of systems approach," *Comput. Methods Programs Biomed.*, vol.191, 105410, 2020, https://doi.org/10.1016/j.cmpb.2020.105410.
[28] K. Clark, B. Vendt, K. Smith, J. Freymann, J. Kirby, P. Koppel, and et al, "The Cancer Imaging Archive (TCIA): maintaining and operating a public information repository.," *J. Digit. Imaging.*, vol.26, pp.1045–1057, 2013, https://doi.org/10.1007/s10278-013-9622-7.
[29] S. Pieper, M. Halle, and R. Kikinis, "3D Slicer", *2004 2nd IEEE International Symposium on Biomedical Imaging: Nano to Macro*, 2005, pp.632–635. https://doi.org/10.1109/isbi.2004.1398617.
[30] P. Cignoni, M. Callieri, M. Corsini, M. Dellepiane, F. Ganovelli, and G. Ranzuglia, "Meshlab: an open-source mesh processing tool.," in: *Eurographics Ital. Chapter Conf.*, 2008, pp. 129–136. http://citeseerx.ist.psu.edu/viewdoc/summary?doi=10.1.1.649.4449.
[31] T.-N. Nguyen, V.-D. Tran, H.-Q. Nguyen, and T.-T. Dao, "A statistical shape modeling approach for predicting subject-specific human skull from head surface," *Med. Biol. Eng. Comput. In Press*, vol.58, pp.2355-2373, 2020. https://doi.org/10.1007/s11517-020-02219-4.
[32] A. Fabri, G.-J. Giezeman, L. Kettner, S. Schirra, and S. Schnherr, "On the design of CGAL a computational geometry algorithms library," *Softw. Pract. Exp.*, vol.30, pp. 1167–1202, 2000, https://doi.org/10.1002/1097-024X(200009)30:11<1167::AID-SPE337>3.0.CO;2-B.
[33] N. Aspert, D. Santa-Cruz, and T. Ebrahimi, "MESH: measuring errors between surfaces using the Hausdorff distance," in: *Proceedings. IEEE Int. Conf. Multimed. Expo, IEEE*, 1978, pp. 705–708. https://doi.org/10.1109/ICME.2002.1035879.
[34] S. Marden and J. Guivant, "Improving the performance of ICP for real-time applications using an approximate nearest neighbour search," *Australas. Conf. Robot. Autom. ACRA.*, 2012, pp. 3–5.
[35] A. Myronenko and X. Song, "Point set registration: Coherent point drifts," *IEEE Trans. Pattern Anal. Mach. Intell.*, vol.32, pp. 2262–2275, 2010, https://doi.org/10.1109/TPAMI.2010.46.
[36] A.S. Householder, "Unitary Triangularization of a Nonsymmetric Matrix," *J. ACM.*, vol.5, pp.339–342, 1958, https://doi.org/10.1145/320941.320947.
[37] S. Koch, "Home telehealth—Current state and future trends," *Int. J. Med. Inform.*, vol.75, pp.565–576, 2006, https://doi.org/10.1016/j.ijmedinf.2005.09.002.

Vi-Do Tran received the Ph.D in BioRobotics, Scuola Superiore Sant'Anna di Pisa, Italy, in 2019. His research interests are in the fields of rehabilitation robotics, assistive technologies, human-robot interaction and biomechanical simulation.

Tien Tuan Dao is Full Professor in Biomedical Engineering and Biomechanics at Centrale Lille Institut, France since 2020. His research interests concern computational biomechanics, knowledge and system engineering, and in silico medicine.

Tan-Nhu Nguyen received the Ph.D in Biomedical Engineering and Biomechanics at Université de technologie de Compiègne, France, in 2020. His current research interest is muscle modeling coupled with serious game for facial rehabilitation.